Dehydration of Sodium Carbonate Decahydrate to Monohydrate in a Fluidized Bed

M. Hartman, V. Veselý, K. Svoboda, and O. Trnka
Institute of Chemical Process Fundamentals, Academy of Sciences of the Czech Republic, 165 02 Prague 6-Suchdol, Czech Republic

Z. Beran
LEAR Corp., 636 00 Brno, Czech Republic

Kinetics of the thermal dehydration of sodium carbonate decahydrate to monohydrate is investigated at temperatures between 15 and 30°C in a batch, fluidized-bed, 140-mm-ID reactor. Effects of particle size, mass of bed, and gas velocity on the dehydration rate are also explored. A simple correlation based on the collected experimental data is developed. The proposed rate law formula makes it possible to estimate the dehydration rate that would be needed to design the performance of a fluidized-bed drying unit. The produced monohydrate is subjected to textural analysis, and pore volume and surface-area data are presented.

Introduction

It has been well established that the removal of sulfur dioxide from flue or waste gas by reaction with "active soda" at moderate temperatures has attractive features (Hartman et al., 1979; Kimura and Smith, 1987; Keneer and Khang, 1993; Kopac et al., 1996). By the term "active soda" we usually mean a porous sodium carbonate produced by the thermal decomposition of sodium hydrogen carbonate (bicarbonate) under appropriate conditions (Bareš et al., 1970). In comparison with calcium oxide, such a solid sorbent reacts with sulfur dioxide almost completely and much more rapidly even at lower temperatures (120–180°C). Our experience as well as that of others (Svoboda et al., 1990; Mocek et al., 1996) indicates that active soda also exhibits a considerable reactivity toward weakly acid NO_x and affinity for difficult penetrative odors.

Aside from the porosity, the surface area of the solid is also substantially increased as a gaseous product evolves in the course of the thermal decomposition. There are causal links between the low temperature of decomposition of the parent materials (precursors) and large surface area (and porosity) and high reactivity of their calcines (Hartman et al., 1978; Hartman and Svoboda, 1985; Borgwardt, 1989; Mai and Edgar, 1989; Irabien et al., 1990; Hartman et al., 1994a,b).

The decomposition reaction is virtually always accompanied with the process of undesirable sintering of the nascent solid product. As micrograin sintering occurs, the surface area is reduced and a significant portion of pore volume can be lost (Borgwardt and Rochelle, 1990; Milne et al., 1990; Hartman et al., 1994a,b, 1997). Research indicates that the calcined product is the most reactive when a certain small fraction of parent material remains undecomposed in the reaction product.

Hu et al. (1986) found that the $NaHCO_3$ particles commence decomposing in a helium stream at approximately 92°C. The rapid rate, that remained high up to high conversions to Na_2CO_3, was attained at 200°C. Corresponding textural data indicated that the surface area and pore volume were greater for the particles decomposed at lower temperatures.

The thermal dehydration of sodium carbonate decahydrate (SCD) takes place in two stages (Waterfield et al., 1968) as follows:

$$Na_2CO_3 \cdot 10H_2O(s) = Na_2CO_3 \cdot H_2O(s) + 9H_2O(g)$$

$$\Delta H^{\circ}_{298} = +52.669 \text{ kJ/mol } H_2O \qquad (1)$$

Correspondence concerning this article should be addressed to M. Hartman.

and

$$Na_2CO_3 \cdot H_2O(s) = Na_2CO_3(s) + H_2O(g)$$
$$\Delta H^{o}_{298} = +58.770 \text{ kJ/mol } H_2O. \quad (2)$$

A transitory occurrence of the metastable heptahydrate cannot be ruled out under specific conditions. As can be seen, the decomposition reactions (Eqs. 1 and 2) are considerably endothermic with the heats of reaction cited earlier. These are appreciably greater than the heat of vaporization of liquid water at 298 K, which amounts to 43.993 kJ/mol (Perry and Chilton, 1973).

The dissociation pressure of sodium carbonate decahydrate can be predicted from an equation developed by Baxter and Cooper (1924):

$$\ln P^{*}_{H_2O} = 25.1719 - \frac{8{,}368.79}{T + 46.45}. \quad (3)$$

Predictions of this equation show that the dissociation pressures of SCD are at 20–25°C, approximately 30% lower than the equilibrium water-vapor pressures on liquid water estimated with the aid of Eq. 4 (Hartman and Trnka, 1993):

$$\ln P^{*}_{H_2O} = 18.1304 - \frac{5{,}041.68}{T}. \quad (4)$$

In the course of the dehydration, the solid phase undergoes deep crystallographic transformation. The original monoclinic lattice of sodium carbonate decahydrate is transformed into the orthorhombic unit of sodium carbonate monohydrate (SCM). Although both the precursor and the product possess only one known crystal structure, the detailed mechanism of the the transformation from the standpoint of crystallography is not entirely clear.

As Eq. 3 predicts, SCD already exhibits appreciable dissociation pressures at room temperatures. Note that SCD already can melt (dissolve) in its crystal water at 32.5–34.5°C (Weast and Astle, 1981). It is known that the porous and reactive product is only formed provided no liquid phase appears in the course of reaction 1.

The fluidized bed with its high heat-transfer rate offers a favorable milieu for carrying out such gas–solid reactions (Yates, 1983; Yates and Simons, 1994). The solid particles it contains are in continuous motion and are normally very well mixed. Occasional "hot/cold spots" are rapidly dissipated and the bed operates in an essentially isothermal and well-controlled mode.

Here we report the results of an investigation of dehydrating the sodium carbonate decahydrate to the monohydrate in a fluidized bed operated in batch manner. In addition to the kinetic experiments, pore-volume and surface-area data were obtained for the solid product in order to evaluate changes in pore texture as a result of reaction.

Experimental Studies

Apparatus

The principal component of the experimental setup was a cylindrical glass column of 140 mm ID ($F = 0.01539$ m^2) and height 0.600 m. The column was equipped with a sandwiching perforated-plate distributor of 5% free area and an orifice diameter of 1.0 mm. Every care was taken to ensure uniform gas (air) distribution within the vessel. Air passed through an oil filter, drier, rotameter, and electric heater before it entered the bottom. Air leaving the column passed through a cyclone and fabric filter. Further details on the apparatus can be found in a recent article of ours (Trnka et al., 2000).

The inlet temperature of fluidization air was measured and controlled by means of a Ni–CrNi thermocouple connected to a PID-type temperature controller. Temperature within the fluidized bed was measured by a thermoelement that was located at about 7 cm above the distributor plate. Humidity of the entering and outgoing air streams was also monitored. The reactor (drier, dehydrator) was operated in a batchwise manner, and solids samples could readily be withdrawn from the bed.

Material, particles

The experiments were performed with the SCD obtained as Fluka Analyzed p.a. Grade. The producer's specifications (Fluka Chemie A.G.) showed purity above 99%. Results of an X-ray power-diffraction analysis confirmed the presence of a single solid component in the sample. The mass fraction of water, z, determined as weight loss at 150°C indicated that the number of mols of water per mol of Na_2CO_3 (ASC), n,

$$n = \frac{M_{Na_2CO_3}}{M_{H_2O}} \cdot \frac{z}{1 - z}, \quad (5)$$

was slightly less than 10. As stoichiometry indicates, $n = 10$ when $z = 0.6296$, and $n = 1$ if $z = 0.1453$.

Using a microscope heated at a rate of 2°C/min, temperature was determined when first signs of crystal melting became noticeable. The measured results are plotted in Figure 1. As can be seen, sodium carbonate hydrates are prone to

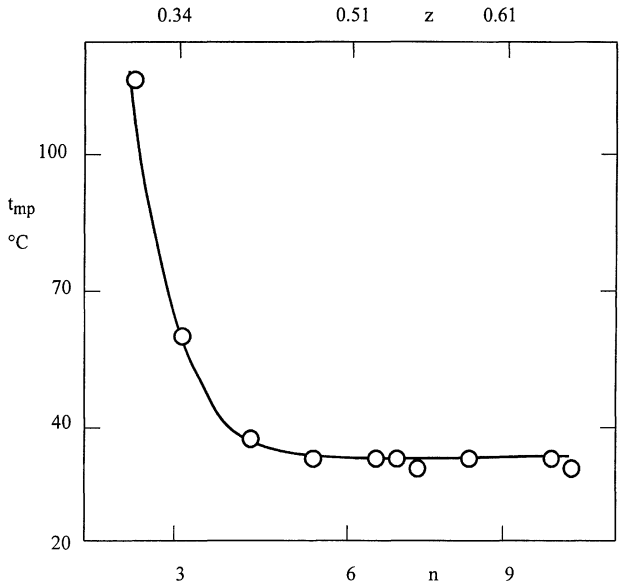

Figure 1. Melting points of sodium carbonate hydrates as a function of water content in solids.
The quantity n is given by Eq. 5.

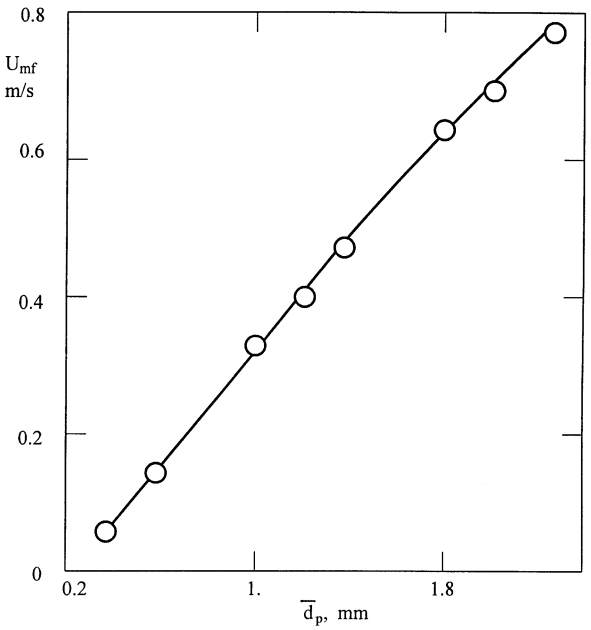

Figure 2. Minimum fluidization velocity of SCD particles measured at 20°C as a function of the mean particle size.

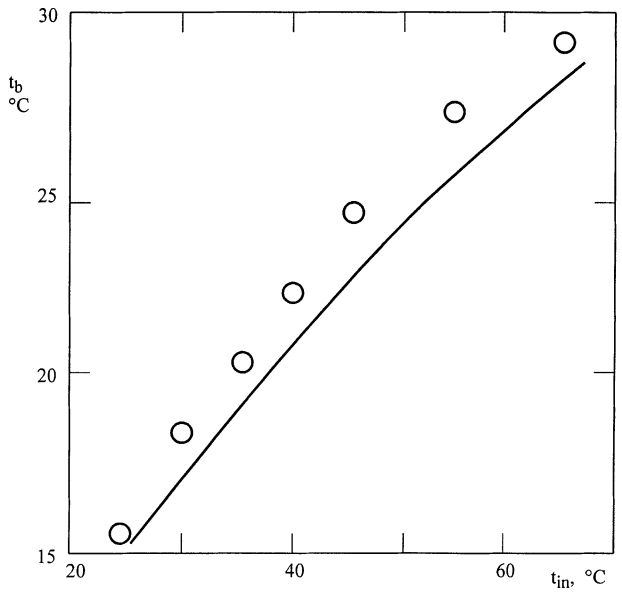

Figure 3. Thermal behavior of the fluidized-bed reactor: bed temperature as a function of temperature of the preheated inlet air.

Initial mass of bed, 2,000 g; $z_o = 0.546$; $\bar{d}_p = 0.8$ mm; $H_{\text{fix}} = 0.18$ m; $U = 0.70$ m/s; ○, experimental data points. Solid line shows the predictions of Eq. 6.

melt at approximately 33°C if the mass fraction of water is greater than about 0.4 (that is, $n = 3.9$.) It is notable that the needed quality of the reaction product deteriorates dramatically when the liquid phase forms in the system. Moreover, wet/sticky particles tend to agglomerate and segregate. Such phenomena usually lead to detrimental defluidization. In order to prevent the SCD particles from melting, the bed temperature in early stages of the dehydration should not be greater than approximately 30°C.

Crushed SCD crystals were sieved using the Czech Standard series of sieves, which is arranged in multiples of approximately 1.25. The mean particle size, $\bar{d}_p$, used in the work is the arithmetic average of the adjacent sieve apertures in the standard series between which a given fraction was collected.

A newer approach, which reflects the dynamic nature of a fluidized bed, was employed to determine the onset of fluidization (Hartman and Coughlin, 1993; Trnka et al., 2000). This technique determines the point of minimum fluidization as the condition where significant rapid pressure fluctuations begin. Measured minimum fluidization velocities are plotted in Figure 2 as a function of the mean particle size, $\bar{d}_p$. The Reynolds numbers corresponding to the measured minimum fluidization velocities are in the range $Re_{mf} = 1.6$–112. This suggests that a transitional flow regime of 0.4–2.2-mm particles of SCD is most likely to occur at the onset of fluidization.

Thermal behavior of the fluidized bed with SCD particles

The thermal dehydration of a batch of the SCD solids can be viewed as an approximately adiabatic process in which heat lost by the entering gas is transferred to the particles to vaporize water. In other words, the heat content of the preheated fluidizing air is the energy source for the dehydrating particles. Then, providing the rate of dehydration is constant, the temperature of bed, T_b, can be expressed as follows:

$$T_b = T_{\text{in}} - \frac{\Delta H^{\circ} r}{V C_{pa}}. \tag{6}$$

At the beginning of the experimental work, a series of experiments were performed to determine the thermal behavior of the reactor at a different inlet temperature of the preheated air. At first, fluidization air ($U < U_{mf}$) was fed into the empty reactor, the temperature of which was less than 33°C. Then a batch of the SCD particles was introduced in the vessel and the air flow rate was adjusted to a desired level. The temperature of the bed reached its steady-state value in a few minutes. Figure 3 shows the behavior of the reaction system for $n > 1$ when the rate of dehydration is constant. As can be seen, dependence of t_b upon t_{in} is slightly curved and the predictions of Eq. 6 are in reasonable agreement with the measured values. The experimental findings presented in Figure 3 were employed in other work, as they make it possible to readily attain the bed temperature of interest.

Kinetics of SCD Decomposition

A weighed amount of sieved SCD particles (1.5–2.0 kg) was charged to the reactor, and the flow rate of air and its temperature were adjusted as mentioned earlier. Small samples of solids were withdrawn from the fluidized bed at regular time intervals in order to determine the content of water in the product. The amount of water in the solids was determined as weight loss at 150°C.

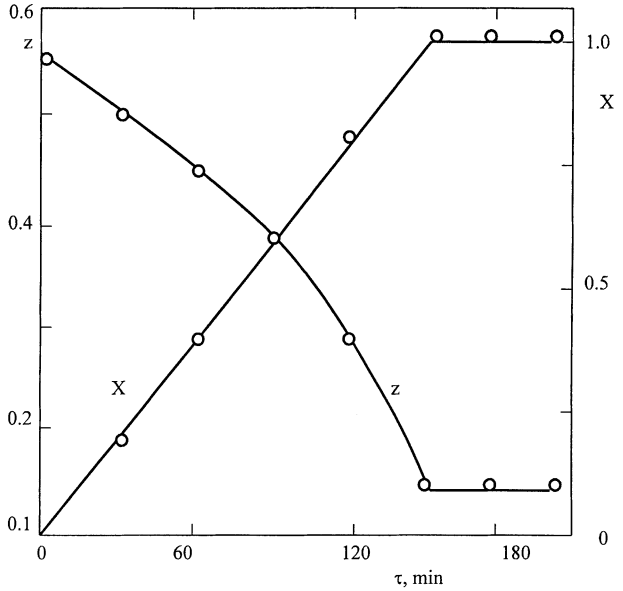

Figure 4. Path of conversion of sodium carbonate dehydrate to monohydrate.

Bed temperature, 22°C; initial mass of bed, 1,500 g; $z_o = 0.56$; $\bar{d}_p = 0.8$ mm; $H_{\text{fix}} = 0.13$ m; ○, experimental data points.

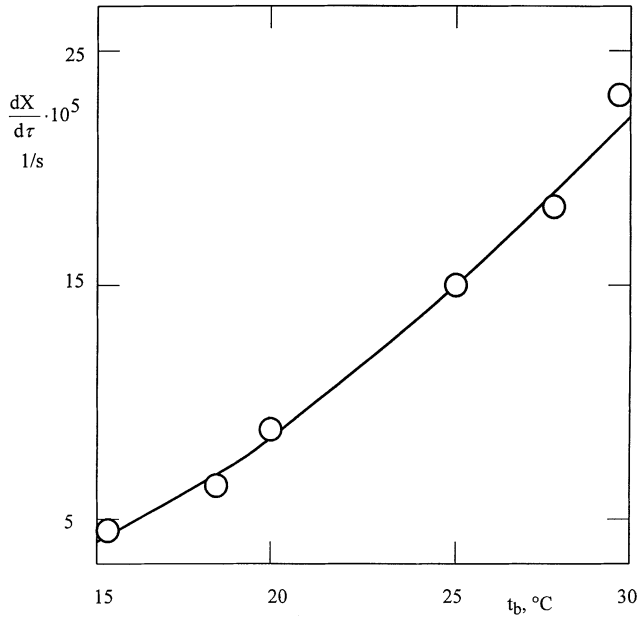

Figure 5. Rate of dehydration of SCD in the fluidized bed at different temperatures.

Static-bed height, $H_{\text{fix}} = 0.18$ m; particle size, $\bar{d}_p = 0.8$ mm; superficial gas velocity, $U = 0.70$ m/s; mean gas residence time, $\bar{\tau}_g = 0.13$ s. Solid line shows the predictions of Eq. 10.

Conversions of the SCD to the monohydrate were calculated from the decrease in weight fraction of water in solids, $z(\tau)$, at any moment of time, and the equation

$$X = \frac{1}{n_o - 1} \cdot \frac{M_{\text{Na}_2\text{CO}_3}}{M_{\text{H}_2\text{O}}} \cdot \frac{z_o - z(\tau)}{(1 - z_o)[1 - z(\tau)]}, \qquad (7)$$

in which $z(\tau) \geq 0.1453$.

The symbols n_o and z_o are the number of mols of water per one mol of Na_2CO_3 and mass fraction of water in the original (initial) sample (at $\tau = 0$), respectively. Complete conversion of $Na_2CO_3 \cdot 10\ H_2O$ ($n_o = 10$, $X = 0$) to $Na_2CO_3 \cdot H_2O$ ($n = 1$, $X = 1$) corresponds to a theoretical decrease in water content of the solid, z, from 0.6296 to 0.1453.

Figure 4 shows the path of dehydration in the course of time at 20°C. It may appear somewhat unexpected that the rate of dehydration, dX/dt, is constant until complete conversion to the monohydrate is attained. This phenomenon suggests that the crystal water is bonded rather weakly to the carbonate. There is an apparent resemblance of the SCD dehydration to a physical process such as the constant-rate drying regime of the solids.

With the aid of Eq. 7, the overall rate, r, in Eq. 6 at which water vapor is released from the bed can be expressed as

$$r = n_{ASC} \cdot (n_o - 1) \cdot \frac{dX}{d\tau}, \qquad (8)$$

where n_{ASC} is the amount of Na_2CO_3 present in the bed, and X is the fractional conversion of the decomposing SCD to the monohydrate given by Eq. 7.

In this work, the rate of dehydration was explored in terms of the bed temperature, air flow rate, and particle size of the decomposing SCD.

Influence of bed temperature

Using 0.8-mm particles, dehydration behavior was explored at bed temperatures between 15.3 and 29.6°C. Corresponding temperatures of the preheated inlet air varied from 25°C to 65°C and can be estimated with the aid of Figure 3. This figure and the results plotted in Figure 1 imply that temperature of the inlet air should be lower than approximately 70°C in order not to bring about any melting action of the solid phase. For ordinary fluidizing conditions, it is commonly accepted (that is, Yates and Simons, 1994) that gas and solids are at the same temperature everywhere within the bed.

Experimental results, as seen in Figure 5, show that the temperature exerted a strong favorable influence on the measured rates of dehydration. When the bed temperature was increased from about 15°C to approximately 30°C, the reaction rate went up nearly five times. This increase can be attributed to the increase in the surface temperature of the particle, resulting in higher dissociation pressure.

The driving force for the conversion of the sodium carbonate decahydrate into the monohydrate can be taken as the difference between the dissociation pressure of SCD and the partial vapor pressure of water in the dehydrating (drying) air. However, a question can arise of how to represent with confidence the mean water-vapor concentration in the gas encountered by the reacting solids within the bed. Research indicates that it is feasible to assume that the gas passes through the fluidized bed in plug flow (Davis and Levenspiel, 1983; Hartman et al., 1988) Thus, the mean concentration of

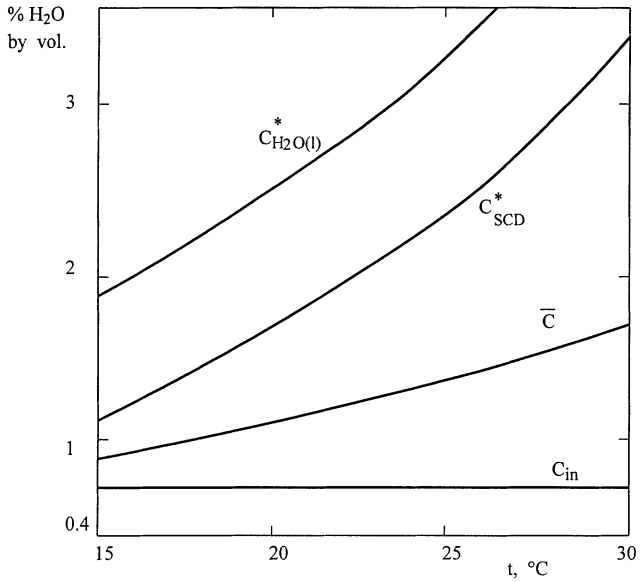

Figure 6. Concentration of water vapor in the gas phase as a function of temperature.

Line C^*_{SCD} shows the equilibrium concentration over SCD predicted by Eq. 3 for ambient pressure; line $\overline{C}$ shows the values given by Eq. 9 provided $C_{out} = C^*_{SCD}$; line $C^*_{H_2O(l)}$ shows the equilibrium concentration over liquid H_2O predicted by Eq. 4 for ambient pressure.

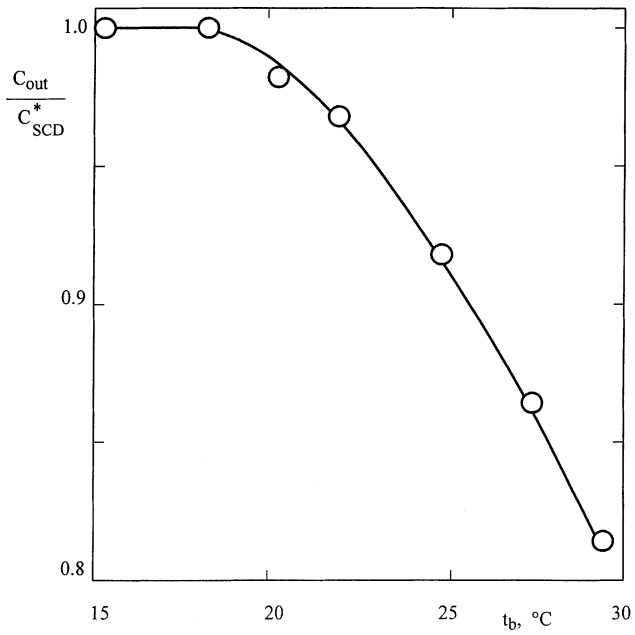

Figure 7. Degree of saturation of the gas phase as a function of the bed temperature.

Experimental conditions are the same as mentioned in the caption for Figure 5.

water vapor, $\overline{C}$, encountered by the decomposing particles at any instant can be expressed as

$$\overline{C} = \frac{C_{out} - C_{in}}{\ln (C_{out}/C_{in})}, \qquad (9)$$

where C_{in} and C_{out} are the concentrations of water vapor in the gas streams entering and leaving the reactor (bed), respectively.

In Figure 6, the ideal course of $\overline{C}$ is depicted as a function of temperature, provided $C_{out} = C^*_{SCD}$, that is, the gas leaving the reactor (bed) is in equilibrium with the decomposing solids of SCD. The vertical distance between curves C^*_{SCD} and $\overline{C}$ suggests a maximum driving force that can theoretically be attained. As visualized, the difference between C^*_{SCD} and $\overline{C}$ increases considerably with temperature. Results plotted in Figure 7 indicate that the approach to equilibrium is quite narrow for mass and heat transfer. If the bed is operated at temperatures below approximately 21°C, the thermodynamic constraints become evident, and it is the carrying capacity of the gas phase that limits the process of dehydration. We should also note that the operation conditions, where $\bar{\tau}_g =$ 0.26 s, were closer to an "intermediate"- or "deep"- bed regime than to a "shallow"-bed state (Hartman et al., 1991).

Influence of particle size and gas velocity

The rate of dehydration was explored using 0.6- and 2.0-mm particles in the range of 0.31–1.05 m/s of the gas superficial velocities. The results obtained with the mass of the 1.5-kg bed are shown in Figure 8. Both lines in this figure are seen to be slightly concave in shape. As is to be expected from a basic engineering point of view, gas velocity exerted considerable favorable influence on the rate of dehydration. We can argue that an increase in gas flow rate increases the rate of dehydration due to a decrease in the gas film resistance surrounding the particle. On the other hand, it should

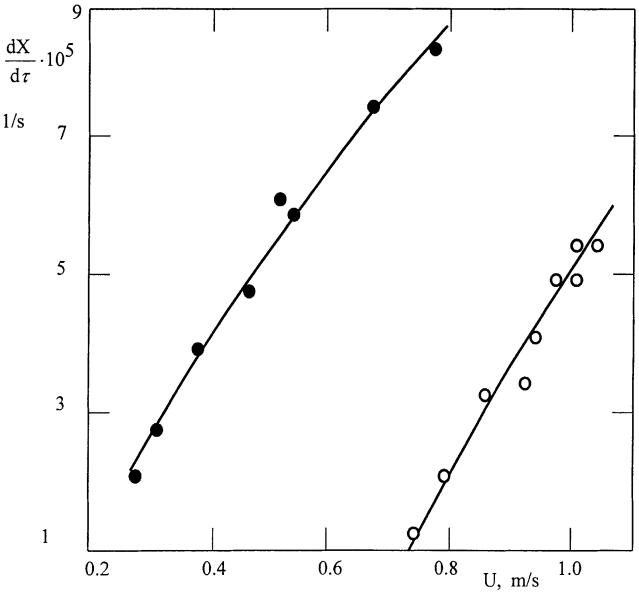

Figure 8. Effect of gas velocity and particle size on the rate of dehydration at 17°C.

● experimental data points measured with 0.6-mm particles; ○, experimental data points measured with 2.0-mm particles; static-bed height, $H_{fix} = 0.14$ cm. Solid lines show the predictions of Eq. 10 for respective particles size.

be noted that the gas leaving the bed was less humid, that is, a greater driving force was achieved when a higher air flow rate was applied.

The effect of particle size is also shown in Figure 8. Again, as is to be expected from simple physical reasoning, the smaller particles were dehydrated more rapidly than the bigger ones at the same gas flow rate. Moreover, the gas exiting the bed of small particles was very close to the saturation point. It is likely that an increase in particle size decreases the rate of dehydration due to reduction in surface area per unit mass of solids.

In general, the preceding results indicate that the most favorable conditions for the thermal dehydration of SCD using a fluidized bed require that the bed of small particles is as hot as safe and still avoids undesirable solid melting. Furthermore, the bed should be as deep as practical and should be operated at higher air flow rates that are compatible with the particle size. However, it should be born in mind that higher gas velocities lead to a certain amount of bypassing, particularly in deep beds, and this reduces the effectiveness of contacting between the phases in the bed.

Determination of rate expression

As follows from the preceding paragraphs, the rate of dehydration is influenced by a number of the system variables. Keeping the given span the temperatures and relatively straightforward reaction chemistry in mind, it appears viable to think of an adequate correlation of the amassed experimental data. This is also facilitated by the fortuitous fact that at the given conditions, the rate of dehydration does not change in the course of reaction.

Having examined several, mostly more involved procedures and relationships, the following simple approach was adopted. It was assumed that the rate of dehydration is governed by two process variables: the driving force, $C^* - \overline{C}$, and excess gas velocity, $U - U_{mf}$, which can be taken as the approximate bubble flow through the bed. The preceding experimental data were fitted by minimizing the standard deviation between the experimental values and the values estimated from the proposed relationship:

$$\frac{dX/d\tau}{C^* - \overline{C}} = 0.0321 \cdot \left(U - U_{mf}\right)^{0.920} + 8.60 \times 10^{-4}. \quad (10)$$

The values of the empirical parameters were computed by the simplex procedure (flexible polyhedron search). Agreement between experiment and the correlation embodied in Eq. 10 appears reasonable, as seen in Figures 5 and 8.

Textural properties of the dehydrated solids

The dehydration of SCD particles at temperatures below the melting point generally takes place without significant change in particle dimensions. This fact, together with the difference in molar volume between $Na_2CO_3 \cdot 10H_2O$ (198.71 cm^3/mol) and $Na_2CO_3 \cdot H_2O$ (55.11 cm^3/mol) indicates that the SCD particle is made much more porous by dehydrating it. Thus, elementary arithmetic leads to the theoretical porosity of $Na_2CO_3 \cdot H_2O$ particles as large as 0.7227 (1.158 cm^3/g) when no shrinkage occurs.

Table 1. Textural Features of Different Sodium Carbonates Prepared by Dehydration/Calcination

Physical Property	$Na_2CO_3 \cdot H_2O$ Prepared from $Na_2CO_3 \cdot 10\,H_2O$ by Dehydration at 25°C	Na_2CO_3 Prepared from $NaHCO_3$ by Calcination at 125°C
Pore Vol. V_p, cm^3/g	0.9718	0.3344
Porosity, e	0.6862	0.4583
Surface Area, m^2/g	11.24	4.09
Median Pore Radius, nm	1.23×10^3	2.22×10^4

Microscope examination revealed (50× magnification) that the $Na_2CO_3 \cdot 10H_2O$ particles were composed of a dense assembly of rather flakelike grains. The original smooth surface of the grains was idented by the dehydration process. After decomposition to $Na_2CO_3 \cdot H_2O$, the SCD grains became smaller, somewhat more spherical in shape, and with substantially more intergrain space.

In several samples ($Na_2CO_3 \cdot H_2O$), prepared by the thermal decomposition of $Na_2CO_3 \cdot 10H_2O$ in the fluidized-bed reactor, physical properties such as pore volume (porosity), BET surface area, and pore-size distribution were determined (Digisorb Analyzer, Micromeritics Auto-Pore).

For the sake of comparison, similar measurements were conducted with Na_2CO_3 particles prepared from sodium hydrogen carbonate ($NaHCO_3$) by calcination at 125°C. The measured results are presented in Table 1 and Figures 9 and 10. As can be seen, the measured pore volume ($e = 0.6862$) was somewhat smaller than its theoretical value ($e = 0.7227$). Nevertheless, it was considerably larger than the porosity ($e = 0.4583$) of anhydrous sodium carbonate prepared from $NaHCO_3$ particles.

Also, the sodium carbonate monohydrate exhibits higher surface area than does Na_2CO_3. Since there is a general cor-

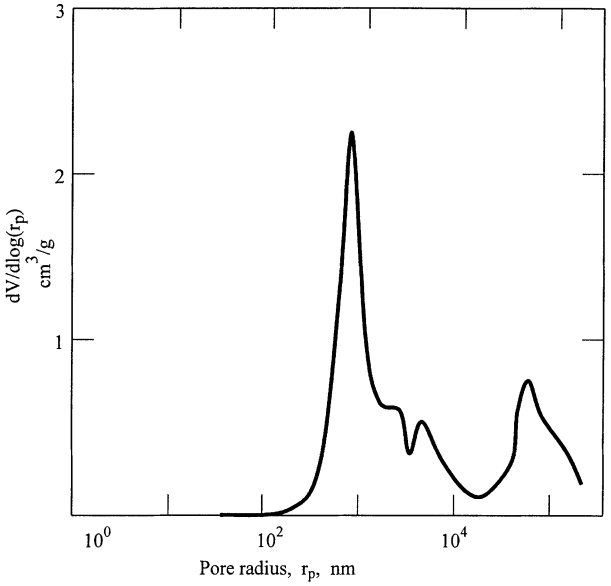

Figure 9. Pore-volume distribution of the $Na_2CO_3 \cdot H_2O$ particles prepared from $Na_2CO_3 \cdot 10H_2O$ by dehydration at 25°C.

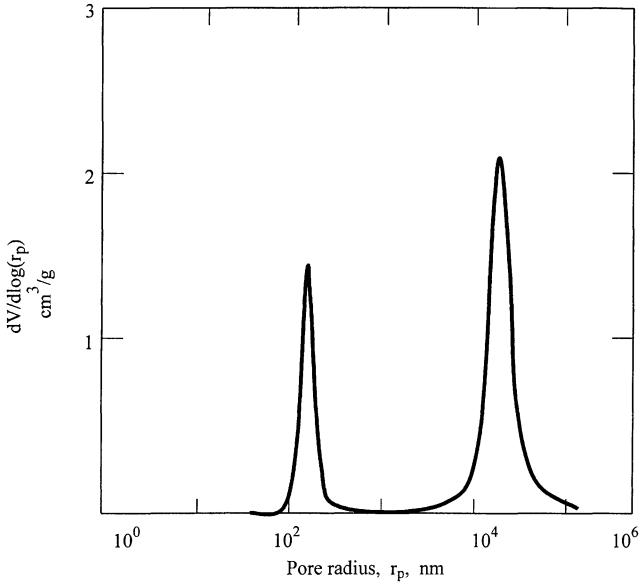

Figure 10. Pore-volume distribution of the Na_2CO_3 particles prepared from $NaHCO_3$ by calcination at 125°C.

relation of reactivity with the textural properties, the higher surface area and greater porosity of the $Na_2CO_3 \cdot H_2O$ particles are expected to lead to increased reaction activity with acidic reactants (Hartman et al., 1978). The distribution curves displayed in Figures 9 and 10 indicate that the pore structure of the $Na_2CO_3 \cdot H_2O$ and Na_2CO_3 particles differ greatly.

Using a small, fixed-bed reactor, experimental measurements were conducted to compare the SO_2 reactivities of $Na_2CO_3 \cdot H_2O$ produced by drying the decahydrate, and the Na_2CO_3 produced by hydrogen carbonate decomposition. The approximately 15–20% longer breakthrough times for the monohydrate beds demonstrated the very high reactivity of the monohydrate prepared from $Na_2CO_3 \cdot 10H_2O$.

The regeneration of the SO_2-loaded sorbent has not been fully resolved yet. It is expected that this spent sorbent can be employed in the glass industry. With respect to the high monohydrate solubility rate, it can also be used to advantage as an important component in laundry products.

Conclusions

In order to prevent the decomposing SCD particles from melting and the subsequent agglomeration, the bed temperature has to be maintained below the 30°C level. The results showed that under such conditions, the dehydration rate was not very rapid. Kinetics was zero order in the $Na_2CO_3 \cdot 10H_2O$ mass, up to practically complete conversion to the monohydrate. The data also showed that the rate decreased when the bed temperature and/or excess gas velocity, $U - U_{mf}$, were reduced and/or, if the particle size was increased. In general, both the experimental findings and the theory strongly suggest that the carrying capacity of the gas is an operation parameter of considerable importance.

Textural analyses proved the dramatic increase in porosity upon converting the $Na_2CO_3 \cdot 10H_2O$ particles to the monohydrate. The reduction in the solid-phase volume due to the reaction leads to a monohydrate porosity as large as 0.686. The surface area of the monohydrate amounts to 11 m^2/g.

Acknowledgment

This research was funded by Grant 203/98/0101 from the Grant Agency CR and Grant A 4072711 from the Grant Agency of the AS CR. The authors thank Mrs. O. Šolcová and Mrs. H. Šnajdaufová for the textural measurements.

Notation

ASC = anhydrous sodium carbonate (Na_2CO_3)
C_{in} = concentration of water vapor in the inlet air, mol fraction
C_{out} = concentration of water vapor in the gas leaving the reactor, mol fraction
C_{pa} = specific heat of air (= 29.19), J/(mol·K)
$C^*_{H_2O}$ = equilibrium concentration of water vapor in the gas phase given by Eq. 4 for ambient pressure, mol fraction
C^*_{SCD} = equilibrium concentration of water vapor in the gas phase given by Eq. 3 for ambient pressure, mol fraction
$\bar{C}$ = mean concentration of water vapor in the gas phase within the bed given by Eq. 9, mol fraction
$\bar{d}_p$ = mean sieve size of solids, m, mm
e = porosity of particle ($= 1 - \rho_p/\rho_s$)
F = cross-sectional area of empty vessel (= 0.015394), m^2
H_{fix} = static bed height, m
ΔH^o = standard heat of reaction, J/mol H_2O
ln = base e or natural logarithm
M_i = molar mass of species ($M_{H_2O} = 18.015$; $M_{Na_2CO_3} = 105.989$; $M_{SCD} = 286.141$), g/mol
n = number of mols of water per mol of Na_2CO_3 in the solid phase
n_o = number of mols of water per mol of Na_2CO_3 in original sample
n_{ASC} = amount of Na_2CO_3 in bed, mol
$P^*_{H_2O}$ = equilibrium pressure of water vapor, kPa
r = overall rate of release of water from bed given by Eq. 8, mol/s
r_p = pore radius, nm
Re_{mf} = Reynolds number at the point of minimum fluidization ($= U_{mf} d_p \rho_f/\mu_f$)
SCD = sodium carbonate decahydrate ($Na_2CO_3 \cdot 10\ H_2O$)
SCM = sodium carbonate monohydrate ($Na_2CO_3 \cdot 10\ H_2O$)
t_b = temperature of bed, °C
t_{in} = temperature of preheated inlet air, °C
t_{mp} = temperature of melting point, °C
T_b = thermodynamic temperature of bed, K
T_{in} = thermodynamic temperature of preheated inlet air, K
U = superficial gas velocity (measured on an empty vessel basis), m/s
U_{mf} = minimum fluidization velocity, m/s
$U - U_{mf}$ = excess gas velocity, m/s
V = flow rate of air ($= FU\rho_m$), mol/s
V_p = pore volume of particle ($= 1/\rho_p - 1/\rho_s$), cm^3/g, m^3/kg
X = fractional conversion of sodium carbonate decahydrate to monohydrate, mol $Na_2CO_3 \cdot H_2O$/mol Na_2CO_3 given by Eq. 7
z = mass fraction of water in solid phase
z_o = initial mass fraction of water in solid phase
(l) = liquid phase
(s) = solid phase

Greek letters

ϵ_{mf} = bed voidage at minimum fluidization
μ_f = fluid viscosity, kg/(m·s)
ρ_f = fluid density, kg/m^3
ρ_m = air density under ambient pressure ($= 12{,}187 \cdot /T$), mol/m^3
ρ_p = apparent (mercury) density of solid reactant, g/cm^3, kg/m^3

ρ_s = true (skeletal, helium) density of solid reactant, g/cm^3, kg/m^3
τ = exposure time, s
$\bar{\tau}_g$ = mean residence time of gas in bed (= $H_{\text{fix}} \cdot \epsilon_{mf}/U_{mf}$), s

Literature Cited

Bareš, J., J. Mareček, M. Mocek, and E. Erdös, "Kinetics of the Reaction Between the Solid Sodium Carbonate and the Gaseous Sulfur Dioxide. III," *Collect. Czech. Chem. Commun.*, **35**, 1628 (1970).

Baxter, G. P., and W. C. Copper, Jr., "The Aqueous Pressure of Hydrated Crystals. II. Oxalic Acid, Sodium Sulfate, Sodium Acetate, Sodium Carbonate, Disodium Phosphate, Barium Chloride," *J. Amer. Chem. Soc.*, **46**, 923 (1924).

Borgwardt, R. H., "Sintering of Nascent Calcium Oxide," *Chem. Eng. Sci.*, **44**, 53 (1989).

Borgwardt, R. H., and G. T. Rochelle, "Sintering and Sulfation of Calcium Silicate-Calcium Aluminate," *Ind. Eng. Chem. Res.*, **29**, 2118 (1990).

Davis, G. F., and O. Levenspiel, "Simple Experimental Method for Finding the Kinetics of Gas-Solid Reactions," *Ind. Eng. Chem. Fundam.*, **22**, 504 (1983).

Hartman, M., J. Pata, and R. W. Coughlin, "Influence of Porosity of Calcium Carbonates on Their Reactivity with Sulfur Dioxide," *Ind. Eng. Chem. Process Des. Dev.*, **17**, 411 (1978).

Hartman, M., J. Hejna, and Z. Beran, "Application of the Reaction Kinetics and Dispersion Model to Gas-Solid Reactors for Removal of Sulfur Dioxide from Flue Gas," *Chem. Eng. Sci.*, **34**, 475 (1979).

Hartman, M., and K. Svoboda, "Physical Properties of Magnesite Calcines and Their Reactivity with Sulfur Dioxide," *Ind. Eng. Chem. Process Des. Dev.*, **24**, 613 (1985).

Hartman, M., K. Svoboda, O. Trnka, and V. Veselý, "Reaction of Sulfur Dioxide with Magnesia in a Fluidized Bed," *Chem. Eng. Sci.*, (Special Issue on ISCRE-10), **43**, 2045 (1988).

Hartman, M., V. Veselý, and K. Svoboda, "On the Bed Expansion in Aggregative Fluidization," *Collect. Czech. Chem. Commun.*, **56**, 882 (1991).

Hartman, M., and R. W. Coughlin, "On the Incipient Fluidized State of Solid Particles," *Collect. Czech. Chem. Commun.*, **58**, 1213 (1993).

Hartman, M., and O. Trnka, "Reactions Between Calcium Oxide and Flue Gas Containing Sulfur Dioxide at Lower Temperatures," *AIChE J.*, **39**, 615 (1993).

Hartman, M., O. Trnka, and V. Veselý, "Thermal Dehydration of Magnesium Hydroxide and Sintering of Nascent Magnesium Oxide," *AIChE J.*, **40**, 536 (1994a).

Hartman, M., O. Trnka, K. Svoboda, and J. Kocurek, "Decomposition Kinetics of Alkaline-Earth Hydroxides and Surface Area of Their Calcines," *Chem. Eng. Sci.*, **49**, 1209 (1994b).

Hartman, M., O. Trnka, and Z. Beran, "Kinetics of the Thermal Decomposition of Hydrated Dolomitic Lime and Sintering of Nascent Calcine," *Chem. Eng. Commun.*, **162**, 199 (1997).

Hu, W., J. M. Smith, T. Dogu, and G. Dogu, "Kinetics of Sodium Bicarbonate Decomposition," *AIChE J.*, **32**, 1483 (1986).

Irabien, A., J. P. Viguri, F. Cortabitarte, and I. Ortiz, "Thermal Dehydration of Calcium Hydroxide," *Ind Eng. Chem. Res.*, **29**, 1599 (1990).

Keneer, T. C., and S. J. Khang, "Kinetics of Sodium Bircarbonate-Sulfur Dioxide Reaction," *Chem. Eng. Sci.*, **48**, 2859 (1993).

Kimura, S., and J. M. Smith, "Kinetics of the Sodium Carbonate–Sulfur Dioxide Reaction," *AIChE J.*, **33**, 1522 (1987).

Kopac, T., G. Dogu, and T. Dogu, "Single Pellet Reactor for the Dynamic Analysis of Gas-Solid Reactions-Reaction of SO_2 with Activated Soda," *Chem. Eng. Sci.*, **51**, 2201 (1996).

Mai, M. C., and T. F. Edgar, "Surface Area Evolution of Calcium Hydroxide During Calcination and Sintering," *AIChE J.*, **35**, 30 (1989).

Milne, C. R., G. D. Silcox, D. W. Pershing, and D. A. Kirchgessner, "Calcination and Sintering Models for Application to High-Temperature, Short-Time Sulfation of Calcium-Based Sorbents," *Ind. Eng. Chem. Res.*, **29**, 139 (1990).

Mocek, K., K. Stejskalová, P. Bach, E. Lippert, Z. Bastl, I. Spirovová, and E. Erdös, "Comparison of the Reactivity of Different Sodium Compounds and $Ca(OH)_2$ Towards SO_2 and Mixtures of SO_2 and NO_x," *Collect. Czech. Chem. Commun.*, **61**, 825 (1996).

Perry, H. R., and C. H. Chilton, "Chemical Engineer's Handbook, 5th ed., McGraw-Hill, Tokyo (1973).

Svoboda, K., V. Veselý, M. Hartman, and K. Jakubec, "Removal of SO_2 and NO_x from Gases with Sorbents Based on Na_2CO_3" (in Czech), *Atmos. Prot.*, (4), 30 (1990).

Trnka, O., V. Veselý, M. Hartman, and Z. Beran, "Identification of the State of a Fluidized Bed by Pressure Fluctuation," *AIChE J.*, **46**, 509 (2000).

Waterfield, C. G., R. G. Linford, B. B. Goalby, T. R. Bates, C. A. Elyard, and L. A. K. Staveley, "Thermodynamic Investigation of Disorder in the Hydrates of Sodium Carbonate." *Trans. Faraday Soc.*, **64**, 868 (1968).

Weast, R. C., and M. J. Astle, *Handbook of Chemistry and Physics*, 62nd ed., CRC Press, Boca Raton, FL (1981).

Yates, J. G., *Fundamentals of Fluidized-Bed Chemical Processes*, Butterworths, London (1983).

Yates, J. G., and S. J. R. Simons, "Experimental Methods in Fluidization Research," *Int. J. Multiphase Flow*, **20** (Suppl.), 297 (1994).

Manuscript received Nov. 22, 2000, and revision received Apr. 26, 2001.